Applied Chemical Engineering (2024) Volume 7 Issue 2
doi: 10.59429/ace.v7i2.5506

ORIGINAL RESEARCH ARTICLE

Investigation of novel organic-based anti-microbial agents with polyolefins

Saleh Alkarri

School of Packaging, Michigan State University, 448 Wilson Road, East Lansing, MI 48824-1223, USA.
orcid.org/0009-0003-3549-9585

***Corresponding author:** Saleh Alkarri, alkarris@msu.edu

ABSTRACT

This study investigated the anti-microbial efficacy of Nouvex N950-9010 MB, an organic-based master batch, when integrated into polypropylene (PP) and high-density polyethylene (HDPE). The focus centers on its effectiveness against two common bacterial strains: *E. coli* K-12 MG1655 and *S. aureus* ATCC 6538P. The master batch was compounded at a 5 wt.% loading concentration with PP and HDPE, and was utilized to create monolayer and multilayer films. The findings reveal significant anti-microbial activity at both 4-hour and 24-hour intervals. SEM analysis confirmed homogeneous mixing and optimal adhesion within the films. Thermal stability, assessed via DSC and TGA, remained consistent, with variations within experimental error margins. Surprisingly, FTIR results indicated no substantial differences between modified and unmodified materials, suggesting that Nouvex N950-9010 MB. preserves material integrity. Mechanical properties, including Izod impact and tensile strengths, remained stable in the modified materials. Moreover, the modified PP and HDPE exhibited improved oxygen and water vapor barrier properties (OTR and WVTR) compared with their neat counterparts. UV spectra validated the non-leachability of Nouvex N950-9010 MB, aligning with the manufacturer's claims. A groundbreaking revelation from the study is that this master batch functions via reactive oxygen species (ROS), marking a pioneering discovery in the field of novel anti-microbial agents. The research demonstrates Nouvex N950-9010 MB's potential as a powerful and safe solution for antimicrobial applications, opening new avenues for further exploration and practical implementation.

Keywords: Anti-microbial activity; *E. coli* K-12 MG1655; *S. aureus* ATCC 6538P; non-leachable; ROS; compounding; dyes; Nouvex N950-9010 MB

ARTICLE INFO

Received: 5 June 2024
Accepted: 26 June 2024
Available online: 1 July 2024

1. Introduction

Microorganic transfer through touching various surfaces is considered one of the most common means by which microorganisms are transferred. For example, when an individual touches a railing, doorknob or other surface with contaminated hands, they transfer the microorganisms present on their hands to the surface, enabling the microorganisms to further transfer to other people if they touch that surface.[1] Subsequently, when anyone else touches the same unclean surface and then touches their nose, eyes or mouth without cleaning their hands, they introduce those microorganisms to the body.[2, 3] For instance, the influenza virus is transferred to the body by rubbing the eyes or nose with contaminated hands.[4, 5] Maintaining cleanliness of hands and sterilizing surfaces are key measures to prevent the spread of microorganisms. Moreover, there is air movement whereby some microorganisms can travel through the air after sneezing or coughing infected droplets that can be inhaled by another person.[6] For example,

Mycobacterium tuberculosis and SARS-CoV-2 are transferred by air movement. Air filtering systems can be beneficial in reducing microbial transmission. Studies have shown that anti-microbial and anti-viral coated air filters are effective in preventing the spread of airborne pathogens.[7] High-specification filters can remove such contamination, which could reduce, not only respiratory infections, but also skin, urinary and gastrointestinal infections transmitted via contaminated hands, infection carriers and close contact.[8,9] Therefore, incorporating such air filtering systems could be a significant measure in controlling microbial spread in a variety of environments.

Bacterial colonization on surfaces poses significant health risks, as these microorganisms can lead to various infections and diseases. The growth of bacteria on surfaces, particularly in healthcare settings, can result in the transmission of pathogens, leading to healthcare-associated infections (HAIs). These infections can have serious side effects, ranging from mild irritations to severe conditions that require hospitalization.[10-12] The risks associated with bacterial contamination are heightened in environments where sanitation is compromised or in places with a high frequency of touching, such as door handles and countertops.[13] To mitigate these risks, it is crucial to implement strategies that decrease bacterial contamination. Regular cleaning and disinfection of surfaces are fundamental; however, using anti-microbial surfaces offers an additional layer of protection. These surfaces are treated with substances that inhibit the growth of bacteria, thereby reducing the risk of microbial transmission.[14] Materials such as copper and its alloys have been shown to possess natural antimicrobial properties, effectively killing a wide range of microorganisms on contact.[15] Incorporating such anti-microbial surfaces in high-touch areas can significantly reduce the potential for bacterial growth and the subsequent spread of infections.[16]

Anti-microbial agents designed for polymer applications are a class of additives that imbue plastics and other polymeric materials with the ability to resist and inhibit the growth of harmful microorganisms. These agents can be broadly categorized into organic and inorganic types, each with distinct mechanisms of action and suitability for different polymer matrices.[17,18] Organic anti-microbial agents often include compounds such as triclosan or silver-based additives that are incorporated into the polymer. Inorganic anti-microbial agents typically involve metals or metal oxides, such as silver, copper or zinc oxide, which can be embedded within the polymer structure or coated on the surface.[19]

Nouvex N950-9010 master batch (MB) represents a significant leap forward in anti-microbial technology. Unlike traditional organic-based anti-microbial products, which typically rely on substances that can be rapidly metabolized or neutralized by microbes, Nouvex N950-9010 MB employs a patented technology that offers a persistent, non-leaching effect.[20] This innovative approach ensures that the anti-microbial properties are not diminished over time, providing long-lasting protection against a wide range of pathogens.[21] What also sets Nouvex N950-9010 MB apart is its ability to integrate directly into materials, rather than merely acting as a surface treatment. This integration ensures that the anti-microbial effect is an inherent feature of the material itself, offering continuous and consistent protection. Furthermore, the Nouvex technology operates mechanically, disrupting the microbial cell membrane on contact. This mode of action is less likely to contribute to anti-microbial resistance, a common concern with chemical-based products. In summary, Nouvex N950-9010 MB distinguishes itself from other organic-based anti-microbial agents through its durable, integrated and non-resistance development properties, making it a versatile and effective solution for enhancing material safety and hygiene.[22]

2. Experimental

2.1. Materials

Polypropylene homopolymer (PP 500P grade) was given by SABIC (Riyadh, Saudi Arabia) as pellets having the following characteristics: melting point 166°C, density 905 kg/m^3 and MFI 3 g/10 min. High density

polyethylene (HDPE IP-10262 grade) was given by Dow (MI, USA) as pellets having the following characteristics: melting point 135°C, density 960 kg/m^3 and MFI 9 g/10 min. NOUVEX N950-9010 MB was obtained as pellets from Croda Inc. (N.J., USA) for both PP and PE materials (IL-3157-PP (20 wt.% in PP) and IL-3157-PE (20 wt.% in PE)).

2.2. Methods

2.2.1. Melt-compounding and injection molding of PP and HDPE with NOUVEX N950-9010 MB

The anti-microbial agents (20 wt.% of NOUVEX N950-9010 in PP and 20 wt.% of NOUVEX N950-9010 in PE) were physically mixed and then compounded during extrusion in a 15 cc micro extruder (co-rotating conical twin screws) at a temperature of 210°C with a speed of 10 rpm for 2 min. Anti-microbial agents were added to PP and HDPE at 5 wt.%. Extrusion compounding resulted in PP and HDPE composites containing the MB additives at the planned level. The neat PP and HDPE (without anti-microbial agents) and PP and HDPE with NOUVEX N950-9010 were injection molded into 25 mm diameter and 1.55 mm thick disks, plus tensile and impact test pieces using a 3.5 cc injection mold. The mold temperature was set at 60°C.

2.2.2 Melt-compounding and cast film extrusion of PP and HDPE with NOUVEX N950-9010 MB

The PP pellets and anti-microbial agents (at a 5 wt.% ratio) were physically mixed and then compounded during extrusion in a Leistriz Twin Screw Extruder (Type MIC 27-GL-26D). The screw diameter was 2.7 cm, with an *L*/*D* ratio of 36/1. The HDPE was processed in a similar manner. The same conditions were used for all materials (processing temperature: 210°C, speed: 10 rpm, residence time: 2 min). The compounded PP pellets (**Figure 1**) were then used to produce the cast film using an RCP-0625 micro extruder equipped with a 20.32 cm flex lip die. The temperature profile was set at 150/170/200/215/210/210/210°C from feed to die, and the resulting films had thicknesses of: Monolayer; (1) PP ~ 15 µm, (2) HDPE ~ 25 µm.

As well as the monolayer films, multilayer films were produced with a layer of both PP and HDPE with thicknesses of: Multilayer: (1) PP ~ 58 µm, (2) HDPE ~ 80 µm.

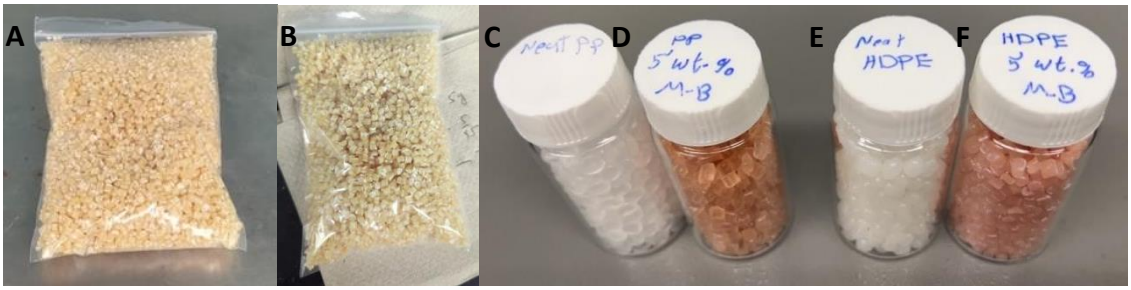

Figure 1. (A) NOUVEX N950-9010 MB for PP, (B) NOUVEX N950-9010 MB for HDPE, (C) Neat PP, (D) PP melt-compounded with 5 wt.% NOUVEX N950-9010 MB for PP, (E) Neat HDPE, (F) PP melt-compounded with 5 wt.% NOUVEX N950-9010 MB for HDPE.

3. Characterization

3.1. Scanning Electron Microscopy (SEM) preparation methods

The extruded films (monolayer and multilayer) underwent characterization using a JEOL 7500F field emission emitter (JEOL Ltd., Tokyo, Japan) for SEM. SEM analysis samples were mounted on aluminum stubs using an adhesive, and followed by coating with a ~ 2.7 nm thick layer of iridium.

3.2. Differential Scanning Calorimetry (DSC)

The melting point and crystallization temperature for the PP and HDPE samples were determined through DSC on a TA Instruments Model Q100 system. A nitrogen flow rate of 70 mL min^{-1} was maintained throughout the measurements. The thermal analysis of the samples spanned a temperature range of -20 to 250°C, with a heating rate of 10°C min^{-1}, and a one-minute hold at each temperature extreme to eliminate any prior effects,

for example processing, crystallization, or thermal or mechanical, history. Subsequently, the samples were cooled to -20°C at a rate of 10°C min^{-1}, then reheated to 250°C at the same rate, and the corresponding thermal responses were recorded. All measurements were conducted in triplicate.

The levels of crystallinity in the PP and HDPE samples were computed based on the heat of fusion values obtained during the second heating cycles, and assessed in accordance with Equation (1):

$$X_c(\%) = \left[\frac{\Delta H_c}{\Delta H_0 . W}\right] x100 \quad \text{(Eq. 1)}$$

where X_c is the crystallinity of the PP or HDPE samples, ΔH_c is the heat of fusion, ΔH_0 is the enthalpy of fusion for 100% crystalline PP [209 J/g][23] or HDPE [293 J/g][24], and W is the fraction (weight) of PP or HDPE in the composite.

3.3. Thermogravimetric Analysis (TGA)

Thermogravimetric analysis (TGA) of the PP and HDPE samples was analyzed using a TA Instruments system (Model Q 50). Each sample, weighing 7 ± 2 mg, was placed in an aluminum pan. The temperature was then incrementally increased from 25 to 600°C at a rate of 10°C min^{-1} under a nitrogen atmosphere with a flow rate of 40 mL min^{-1}. The analysis was performed in triplicate for all samples.

3.4. Fourier-Transform Infrared Spectroscopy (FTIR)

FTIR spectra were recorded with a Shimadzu IR Prestige-21 FTIR spectrophotometer (Shimadzu Co., Columbia, MD) equipped with an attenuated total reflection attachment (PIKE Technologies, Madison, WI). Each sample had 64 scans recorded at a resolution of 4 cm^{-1} in the spectral range of 4000–400 cm^{-1}.

3.5. Melt Flow Index (MFI)

The melt flow index (MFI) analysis of the PP and HDPE samples followed the guidelines given in ASTM D1238-20 and was conducted using a Ray-Ran MK 2 advanced microprocessor system. The analysis was carried out under specific conditions, with a barrel temperature set at 230°C and the piston weight calibrated to 2.16 kg. Each 5 g sample underwent preheating for 7 minutes, followed by cutting at 1-minute intervals and recording the relative weight. This procedure was repeated seven times for each specimen. The results, including the mean and standard deviation, were then reported.

3.6. Density

The density of melt-compounded and injection molded PP and HDPE with the anti-microbial agents was measured using the density gradient method in accordance with ASTM D 1505, Appendix X1, Section 7.2.3 (Ray Ran Auto Density Gradient Column, Warwickshire, UK). A density-gradient range between 0.79 to 1.11 g/cm^3 was prepared using a solution of isopropanol-diethylene glycol. Three replicate 1 cm diameter disks were prepared and placed in the density gradient column, with recording of the samples' densities.

3.7. Barrier properties

3.7.1. Oxygen Transmission Rate (OTR)

The OTR of PP and HDPE film samples (two replicates of each sample produced by the cast film extruder) was assessed at 23°C and 50% relative humidity using an Ox-Tran system (model 2/22, Mocon Inc., MN, USA) following the procedures given in ASTM D3985.

3.7.2. Water Vapor Transmission Rate (WVTR)

The WVTR of PP and HDPE film samples (two replicates of each sample produced by the cast film extruder) was determined at 37.8°C and 90% relative humidity using a Permatran-W system (Model 3/34, Mocon Inc., MN, USA) following the guidelines specified in ASTM F1249. The WVTR calculation involved multiplying the film sample thickness by the corresponding water vapor transmission value.

3.8. Mechanical properties

Izod impact and tensile test pieces were allowed to stabilize at room temperature for a minimum of 40 hours before undergoing testing.

3.8.1. Izod impact

The impact bars were notched using a notch cutter (TMI 22-05, USA) and, after notching, were left at room temperature for an additional 40 hours. Impact strength was assessed in accordance with ASTM D256 utilizing Ray-Ran test equipment with a 5.417 J hammer pendulum. Each test used five replicate specimens.

3.8.2. Tensile properties

The tensile testing was conducted on an Instron system (model 5565, MA, USA) following the procedure in ASTM D638-14 (type V test pieces) at a speed of 10 mm/min. Each test used five replicate specimens.

3.9. UV-visible spectrophotometry — Leachability

PP MB and PE MB. (20 pellets of each material loaded with 20 wt.% NOUVEX N950-9010 MB.), PP compounded with 5 wt.% PP MB, and HDPE compounded with 5 wt.% PE MB. sample (20 pellets) were immersed in 20 mL glass vials containing 5 mL of deionized (DI) water. Each sample was subjected to biaxial rotation along the x-axis using a mini-rotator (Benchmark Scientific, Roto Mini Plus R 2024, Sayreville, NJ, USA) at a speed of 20 rpm for 24 hours. Subsequently, 3 mL of the DI water was taken using a micropipette and subjected to ultraviolet and visible light transmission analysis as per ASTM E169-16. This analysis was performed with a UV-visible spectrophotometer (model UV-1800, Shimadzu Corporation, Kyoto, Japan). Three replicates of each sample were scanned in the wavelength range of 200 to 800 nm at a rate of 480 nm per minute.

3.10. Anti-microbial test method

E. coli K-12 MG1655 and *S. aureus* ATCC 6538P (American Type Culture Collection, Manassas, VA) served as the test strains for assessing the anti-microbial efficacy of the films in all experiments. The initial culture was preserved at -80°C in a ThermoFisher TSX400 system and streaked onto Tryptic Soy Agar (TSA) plates (BBL/Difco, Sparks, MD, USA). Following a 37°C incubation for 24 hours, a single colony was chosen and transferred to 5 mL of Tryptic Soy Broth (TSB) (BBL/Difco, Sparks, MD, USA), then cultured at 37°C for 18 hours. Post-incubation, 1 mL of the culture underwent centrifugation at RCF of 13,000 x g for 5 minutes using a Fisher Scientific accuSpin micro 17 R centrifuge, and the supernatant was discarded. The cells were resuspended in 1 mL of phosphate-buffered saline (PBS, Crystalgen, Innovation for Science, Commack, NY, USA) through vortexing. The resulting cell suspension was transferred to a 15 mL tube, with 11.5 mL of PBS added. The ISO 22196 standard test method for anti-bacterial efficacy, widely recognized as the industry's most commonly employed approach, outlines an in-vitro procedure for evaluating the anti-bacterial impact on treated plastics and other impermeable surfaces (**Figure 2**). This method quantitatively assesses the biocidal or bacteriostatic effects through direct contact between a liquid bacterial culture and surfaces subjected to control or test conditions. In essence, the protocol involves the application of a specified concentration and volume of *E. coli* or *S. aureus* inoculate onto the presumed anti-microbial surface. The surface is then covered with a plastic film, placed in a Petri dish, and incubated for 24 ± 1 hr at 35 ± 1°C with a relative humidity of not less than 90%. The recovery of bacteria from the test specimens takes place immediately after inoculation for control surfaces and after 24 hr of incubation for both control and test surfaces, achieved by introducing a neutralizing solution. Subsequent to bacteria retrieval from the test specimens, they undergo serial dilution and are plated on nutrient agar. While this standard method has been proven reliable for assessing the biocidal activity of active materials and surface coatings, it has been acknowledged that it may not precisely replicate real-world conditions due to its artificial experimental parameters, such as temperature, incubation conditions and relative humidity. Consequently, applying of results to authentic industrial or clinical settings can pose

challenges. Neat PP and HDPE films served as "negative" control samples. Additionally, the anti-microbial activity of various PP and HDPE composite films was individually assessed.

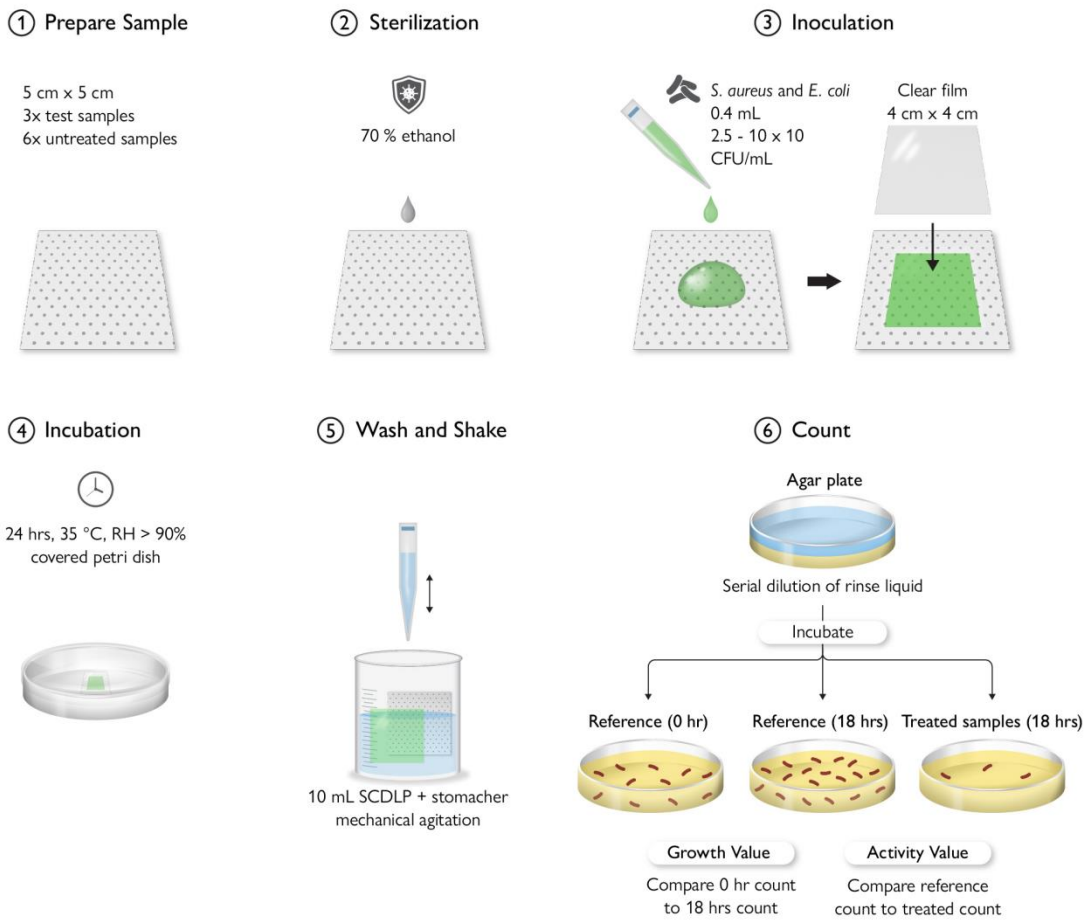

Figure 2. An illustration of the ISO 22196 (measurement of anti-bacterial activity on plastics surfaces) test procedure. Reproduced from ref. [25], open access. Copyright (2023) Alkarri, S.; Bin Saad, H.; Soliman, M.

3.11. Confocal microscopy to study the anti-microbial mechanism

E. coli K-12 MG1655 was employed in the tests to assess and compare the anti-microbial mechanisms of melt-compounded and extruded PP and HDPE films with the anti-microbial agents in both monolayer and multilayer forms. The monolayer extruded film had the anti-microbial agent distributed on all materials as a single layer, while the multilayer of two layers (or more depending on the application) had the compounded anti-microbial agents on the external layer of the film to provide the anti-microbial property. The initial step involved introducing *E. coli* onto the surface of Tryptic Soy Agar (TSA) solid medium, followed by overnight incubation at 37°C. Subsequently, individual colonies were selected and transferred into Tryptic Soy Broth (TSB) liquid medium. The bacterial solution was then agitated at 220 rpm overnight under aerobic conditions using a MaxQ400 instrument (ThermoFisher). The optical density of the resulting bacterial solution was determined, resulting in an OD 600 nm [OD_{600}] value of 0.92, corresponding to approximately 10^5 colony-forming units/mL (CFU/mL).

Confocal fluorescence images were captured using an Olympus FluoView 1000 Confocal Laser Scanning Microscope configured on an automated IX81 inverted microscope with a 60x Plan Apo N oil objective lens (NA 1.42). Olympus FV10-ASW software (version 4.02.03.06) was used for image acquisition and analysis. ROS-positive bacteria were identified by exciting carboxy-H_2DCFDA with a 488 nm argon laser line and recording the green fluorescence emission through a 505 nm long-pass emission filter. Hoechst fluorescence

was excited using a 405 nm diode laser and passed through a blue 430–470 nm band-pass filter before recording. Simultaneously, transmitted light brightfield images of the bacteria were recorded using the 488 nm laser line.

Metal, metal oxide and metal hydroxide nanoparticles have the capability to generate ROS in interacting cells. Čapek and Roušar have extensively reviewed the chemical aspects of metallic nanoparticles.[26] A 250 mL aliquot of each bacterial sample was labeled with 100 mM carboxy-H_2DCFDA (2.5 mL of 10 mM carboxy-H_2DCFDA) and 20 mM Hoechst solution (5 mL of 1 mM Hoechst solution) simultaneously. After a 30-minute incubation at 37°C, the bacterial samples were centrifuged, the supernatant was removed, and the bacterial pellets were resuspended in 40 mL of deionized water for confocal microscopy imaging. Positive ROS detection was shown by green fluorescence of the treated bacteria.

A 250 mL aliquot of a control bacterial sample was incubated with 400 mM TBHP (4 ml of 25 mM TBHP) for 90 minutes at 37°C to provide a positive ROS control. The TBHP treated samples were then labelled simultaneously with 100 mM carboxy-H_2DCFDA and 20 mM Hoechst solution for 30 minutes at 37°C. After centrifugation, removal of the supernatant, and resuspension in 40 mL of deionized water, the bacterial samples were imaged by confocal microscopy (**Figure 3**).[27] An average of ten confocal fluorescence images were collected and analyzed for each sample using Image J software. Positive ROS-labeled cells (shown in green) were identified using the "multi-point" feature in Image J software. The total number of ROS-labeled cells was then counted for each image, to yield the average number of ROS-positive cells for each set of samples which was reported.

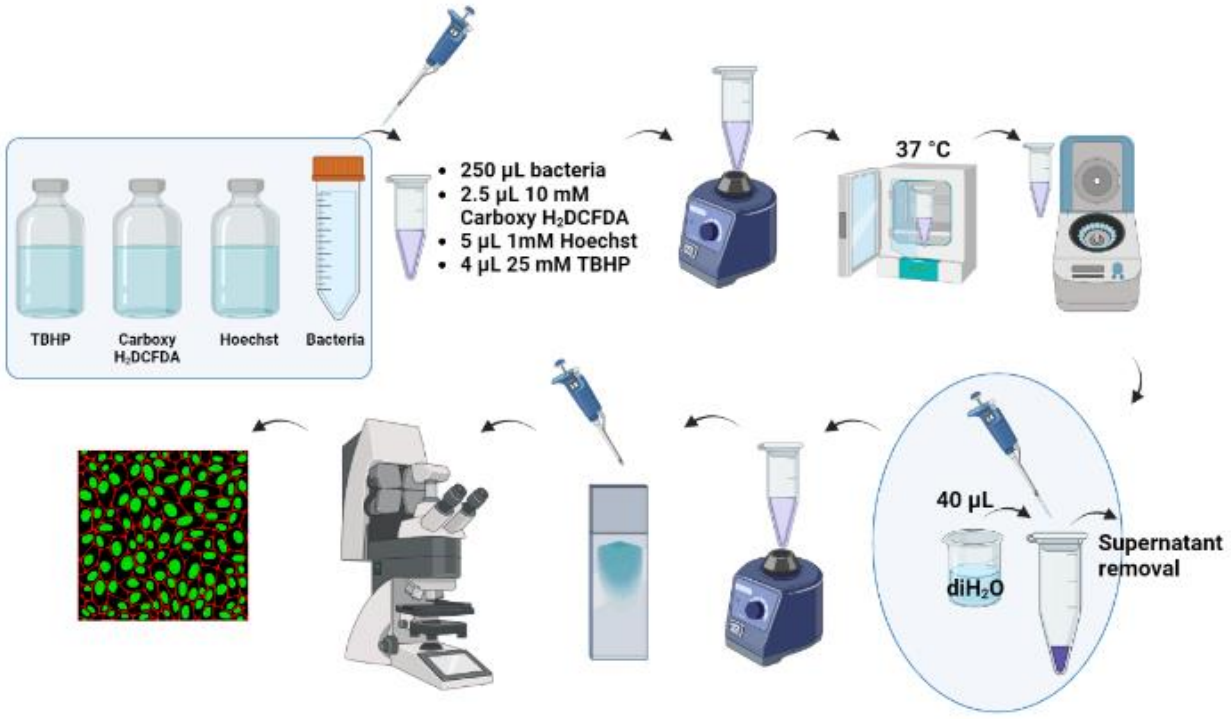

Figure 3. Carboxy-H_2DCFDA staining process. Reproduced from ref. [27], open access. Copyright (2024) Alkarri, S.; Frame, M.; Cairney, J.; Maddan, L.; Kim, J.; Rayner, J.[27]

3.12. Experimental design and statistical analysis

A 2x2 factorial experiment was employed to explore the efficacy of non-leachable organic- based anti-microbial agents (NOUVEX N950-9010 MB) based on the method of incorporation (compounding and film extrusion as monolayer and multilayer) in relation to *E. coli* K-12 MG1655 and *S. aureus* ATCC 6538P. A minimum of three biological replicates were used for all experiments. Variations in *E. coli* K-12 MG1655 cell density resulting from direct exposure to (1) neat PP and HDPE films (negative control), and (2) PP and HDPE

film (monolayer and multilayer) incorporating anti-microbial agents were compared at 0, 4 and 24 hours using Tukey's honest significant difference test and Student's t-test at a 95% confidence level ($p \leq 0.05$). Interactions involving the type of anti-microbial agent, method of incorporating anti-microbial agent with PP and HDPE (compounding, film extrusion as monolayer and multilayer), and anti-microbial activity were scrutinized through a 4-way analysis of variance (ANOVA) using Origin 2022b software (ver. 9.9.5.167: OriginLab Corporation, Massachusetts, USA).

4. Results and discussion

4.1. SEM characterization of cast film extrusion

4.1.1. Monolayer

The cross-sectional SEM images of melt-compounded PP and HDPE with 5 wt.% NOUVEX N950-9010 MB as monolayer films are presented in (**Figure 4**).

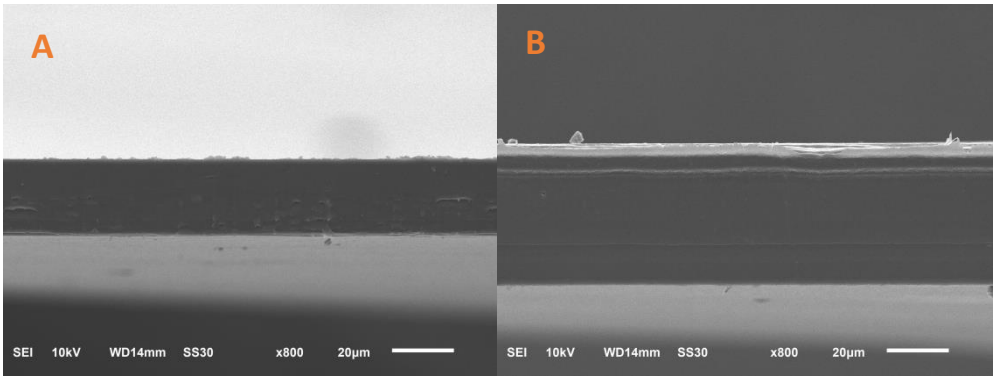

Figure 4. The cross-sectional SEM images of monolayer films for (A) PP compounded with 5 wt.% NOUVEX N950-9010 MB, and (B) HDPE compounded with 5 wt.% NOUVEX N950-9010 MB.

The cross-sectional SEM images of melt-compounded PP and HDPE with 5 wt.% NOUVEX N950-9010 MB through a monolayer film confirmed a well-defined, homogeneous and uniform layer of the compounded and extruded PP (**Figure 4.A**) and HDPE films (**Figure 4.B**) with a layer thickness of ~ 15 and ~ 25 µm, respectively.

4.1.2. Multilayer

The cross-sectional SEM images of melt-compounded PP and HDPE with 5 wt.% NOUVEX N950-9010 MB as multilayer films are presented in (**Figure 5**).

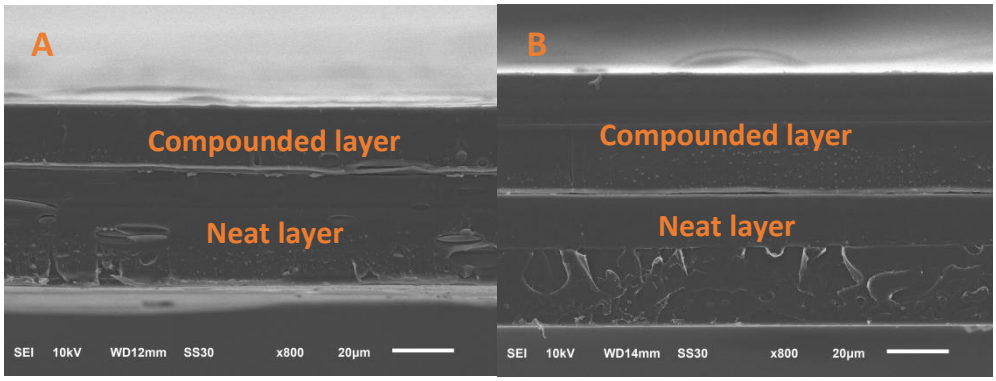

Figure 5. SEM images of multilayer films for (A) PP compounded with 5 wt.% NOUVEX N950-9010, and (B) HDPE compounded with 5 wt.% NOUVEX N950-9010.

The cross-sectional SEM images of melt-compounded PP and HDPE with 5 wt.% NOUVEX N950-9010 MB as a multilayer film structure confirmed a well-defined, homogeneous and uniformly adhered multilayer system of the neat PP layer (~ 40 µm in thickness) and the compounded PP layer (~ 18 µm in thickness), represented in (Figure 5.A), and the neat HDPE layer (~ 40 µm in thickness) and the compounded HDPE layer (~ 30 µm in thickness), represented in (**Figure 5.B**). The middle line represents the joining of the two layers together as this system was produced without a tie layer.

4.2. Differential Scanning Calorimetry (DSC)

The thermal properties of various PP and HDPE samples obtained through DSC are presented in (**Figure 6**) and summarized in (**Table 1**).

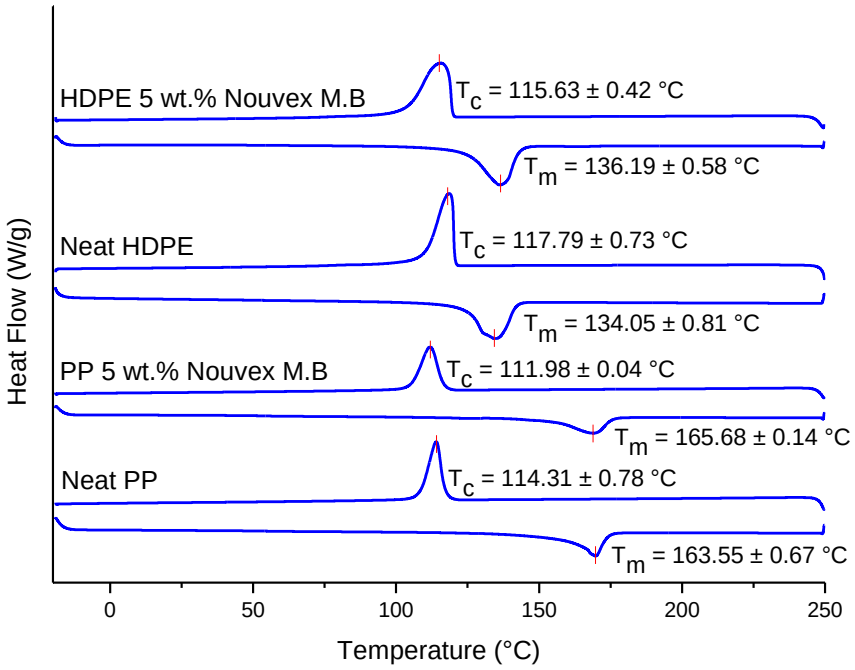

Figure 6. The DSC values of various PP and HDPE samples.

The melting temperatures (T_m) and the crystallization temperatures (T_c) of both the neat PP and neat HDPE samples were comparable to their modified samples with the addition of the 5 wt.% of Nouvex N950-9010 MB. The T_m of the melt-compounded PP with 5 wt.% of Nouvex N950-9010 MB was slightly higher (165.68 ± 0.14°C) than the neat PP sample (164.70 ± 0.67°C), and the melt-compounded HDPE with 5 wt.% of Nouvex N950-9010 MB was also slightly higher (136.19 ± 0.58°C) than the neat HDPE sample (134.05 ± 0.81°C). However, the T_c of the melt-compounded PP with 5 wt.% of Nouvex N950-9010 MS was slightly lower (111.98 ± 0.04°C) than the neat PP sample (114.31 ± 0.78°C), and the T_c of the melt-compounded HDPE with 5 wt.% of Nouvex N950-9010 MB was also slightly lower (115.63 ± 0.42°C) than the neat HDPE sample (117.79 ± 0.73°C).

Table 1. The crystallinity of various PP and HDPE samples obtained from DSC measurements.

Samples	ΔH_m [J/g]	T_m [°C]	T_c [°C]	*Crystallinity* [%]
Neat PP	88.99 ± 1.65	164.70 ± 0.67	114.31 ± 0.78	42.58 ± 0.61
PP 5 wt.% NOUVEX N950-9010 MB (compounded)	72.98 ± 1.88	165.68 ± 0.14	111.98 ± 0.04	33.17 ± 1.65
Neat HDPE	201.90 ± 1.27	134.05± 0.81	117.79 ± 0.73	68.91 ± 0.83
HDPE 5 wt.% NOUVEX N950-9010 MB (compounded)	228.40 ± 3.28	136.19 ± 0.58	115.63 ± 0.42	74.05 ± 3.68

The crystallinity percentages of the melt-compounded PP with 5 wt.% of Nouvex N950-9010 MB samples (33.17 ± 1.65%) were lower than the neat PP sample (42.58 ± 0.61%). Similarly, the crystallinity percentages of the melt-compounded HDPE with 5 wt.% of Nouvex N950-9010 MB samples (74.05 ± 3.68%) were higher than the neat HDPE samples (68.91 ± 0.83%), as calculated in (**Table 1**).

Overall, the thermal properties data obtained from the DSC analysis showed minor differences in both studied cases of melt-compounded PP and HDPE with 5 wt.% of Nouvex N950-9010 MB compared with their neat PP and HDPE cases in terms of T_m and T_c, but a very noticeable difference was observed in the crystallinity percentages. This finding aligns with previous studies. For instance, Gu at el. investigated the effect of peroxide on HDPE and HDPE/PP blends using differential scanning calorimetry and X-ray diffraction techniques. Their results also highlighted changes in crystallinity due to the presence of peroxide.[28] Therefore, the observed variations in crystallinity percentages are consistent with existing literature, emphasizing the unique behavior of Nouvex N950-9010 MS in these polymer blends.

4.3. Thermogravimetric Analysis (TGA)

The thermal properties of PP and HDPE samples obtained through TGA are presented in (**Figure 7**), and the temperatures for 5% weight loss are listed in (**Table 2**).

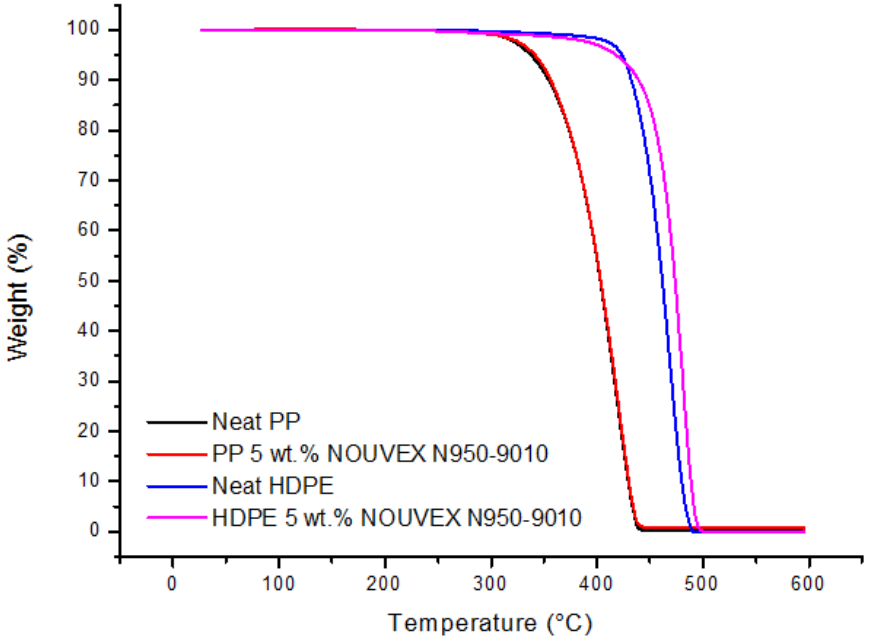

Figure 7. The TGA values of various PP and HDPE samples.

The thermal degradation phase for both neat PP and PP blended with 5 wt.% of Nouvex N950-9010 MB occurred between 300 and 430°C, and for both neat HDPE and HDPE blended with 5 wt.% of Nouvex N950-9010 MB it occurred between 450 and 500°C, as shown in (**Figure 7**).

Table 2. The temperature at which various PP and HDPE samples underwent 5% weight loss as determined via TGA measurements.

Sample	The temperature at which 5% weight loss occurred (°C)
Neat PP	337.37 ± 3.27
PP 5 wt.% NOUVEX N950-9010 MB (compounded)	341.39 ± 4.34
Neat HDPE	423.53 ± 5.34
HDPE 5 wt.% NOUVEX N950-9010 MB (compounded)	418.01 ± 5.02

For the melt-compounded PP with 5 wt.% of Nouvex N950-9010 MS, the overall TGA curve representing the weight loss overlapped with that of the neat PP. However, the temperature for 5% weight loss was 341.39 ± 4.34°C which was higher than the next PP 5% weight loss at 337.37 ± 3.27°C, as listed in (**Table 2**).

The TGA curves obtained for the neat and modified HDPE samples were slightly different. The temperature where 5% weight loss was reached for melt-compounded HDPE with 5 wt.% of Nouvex N950-9010 MB was 418.01 ± 5.02°C, which was higher than the neat PP 5% weight loss at 423.53 ± 5.34°C.

Overall, the thermal stability with the addition of 5 wt.% of Nouvex MB to both PP and HDPE was improved compared with the neat PP and HDPE, as shown in (**Figure 7**).

4.4. Fourier-Transform Infrared Spectroscopy (FTIR)

The FTIR spectra of various PP and HDPE samples are presented in (**Figure 8**).

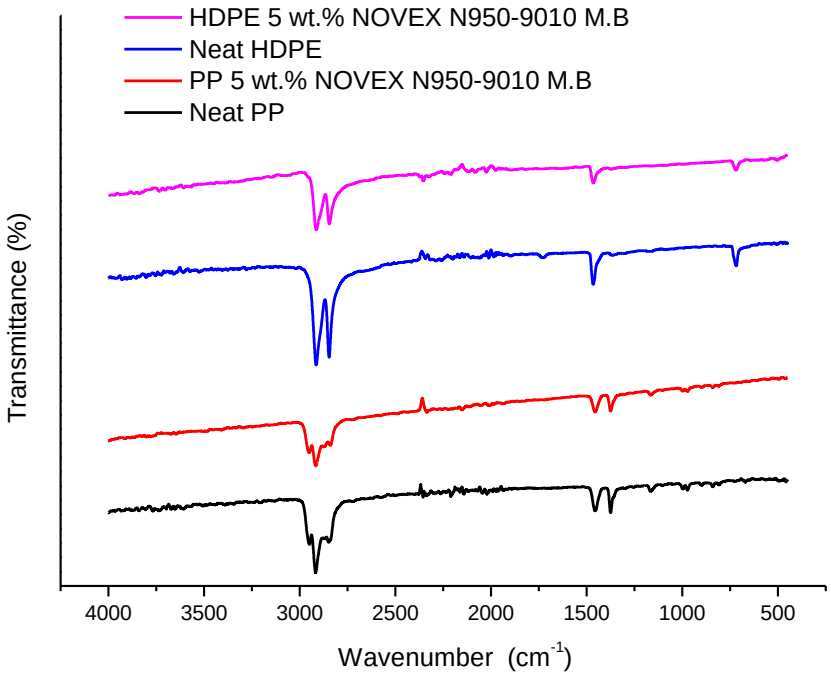

Figure 8. The FTIR spectra of various PP and HDPE samples.

The transmittance curves of the neat PP and HDPE monolayer films with their respective compounded blends at 5 wt.% Nouvex MB were very similar. The peaks around 2800–3000 cm^{-1} represent the alkane C-H stretching, and the peaks around 1450–1465 cm^{-1} represent the alkane C-H bending.

4.5. Melt Flow Index (MFI) and density

The MFI and density values of various PP and HDPE samples are presented in (**Table 3**).

Table 3. The MFI and densities values of various PP and HDPE samples.

Samples	*MFI* [g/10 min]	*Density* [g/CC]
Neat PP	2.953 ± 0.033	0.927 ± 0.004
PP 5 wt.% NOUVEX N950-9010 MB	3.487 ± 0.108	0.931 ± 0.004
Neat HDPE	8.992 ± 0.276	0.934 ± 0.012
HDPE 5 wt.% NOUVEX N950-9010 MB	8.510 ± 0.199	0.928 ± 0.091

The MFI (measured in g/10 min) for the melt-compounded PP with 5 wt.% of Nouvex N950-9010 MB was 3.487 ± 0.108, which was higher compared with the neat PP (2.953 ± 0.033). The MFI for the melt-compounded HDPE with 5 wt.% of Nouvex N950-9010 MB. was 8.510 ± 0.199 g/10 min which was lower compared with the neat HDPE (8.992 ± 0.276 g/10 min).

The density (measured in g/CC) for the melt-compounded PP with 5 wt.% of Nouvex N950-9010 MB was 0.931 ± 0.004 which was slightly higher compared with the neat PP (0.927 ± 0.004). The MFI for the melt-compounded HDPE with 5 wt.% of Nouvex N950-9010 MB was 0.928 ± 0.091 which was lower compared with the neat HDPE (0.934 ± 0.012).

In summary, the MFI and the density measurements for the neat and modified PP and HDPE samples were similar, as listed in (**Table 3**).

4.6. Barrier properties

4.6.1. OTR and WVTR

The OTR and WVTR values of various PP and HDPE samples are presented in (**Figure 9**).

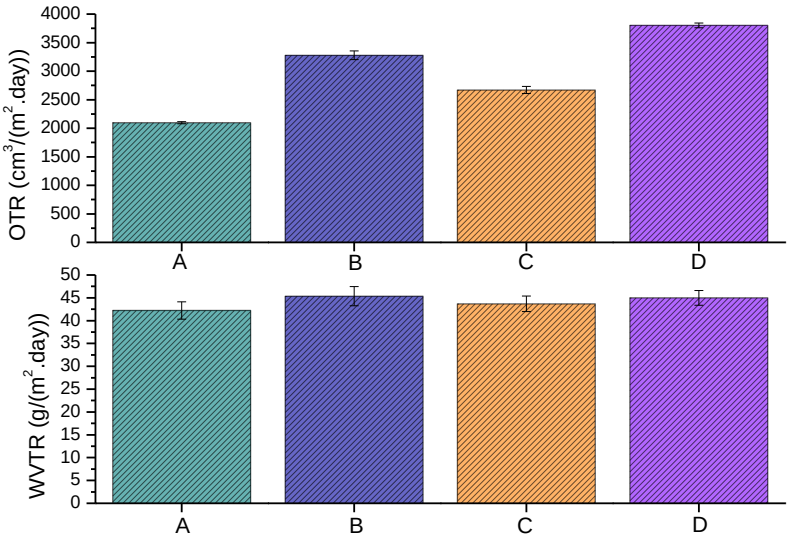

Figure 9. The WVTR and OTR of each graph represent the following samples (on the x axis); (A) neat PP, (B) PP blended with 5 wt.% NOUVEX N950-9010 MB, (C) Neat HDPE, (D) HDPE blended with 5 wt.% NOUVEX N950-9010 MB.

The WVTR (measured in g/(m^2•day)) for the melt-compounded PP with 5 wt.% of Nouvex N950-9010 MB was 45.34 ± 2.1, which was higher compared with the neat PP at 42.23 ± 1.90. The WVTR (measured in g/(m^2•day)) for the melt-compounded HDPE with 5 wt.% of Nouvex N950-9010 MB was 44.98 ± 1.6 which was higher than the neat HDPE at 43.67 ± 1.7.

The OTR (measured in cm^3/(m^2•day)) for the melt-compounded PP with 5 wt.% of Nouvex N950-9010 MB was 3278.68 ± 76.46 which was higher compared with the neat PP at 2098.60 ± 18.84. The OTR (measured in cm3/(m^2•day)) for the melt-compounded HDPE with 5 wt.% of Nouvex N950-9010 MB was 3800.45 ± 41.29, which was higher than the neat HDPE at 2668.38 ± 62.25.

Overall, the addition of 5 wt.% of Nouvex N950-9010 MB improved the barrier properties of both WVTR and OTR for PP and HDPE samples, as shown in (**Figure 9**).

4.7. Mechanical properties

4.7.1. Izod impact

The Izod impact strength of various PP and HDPE samples are presented in (**Figure10**).

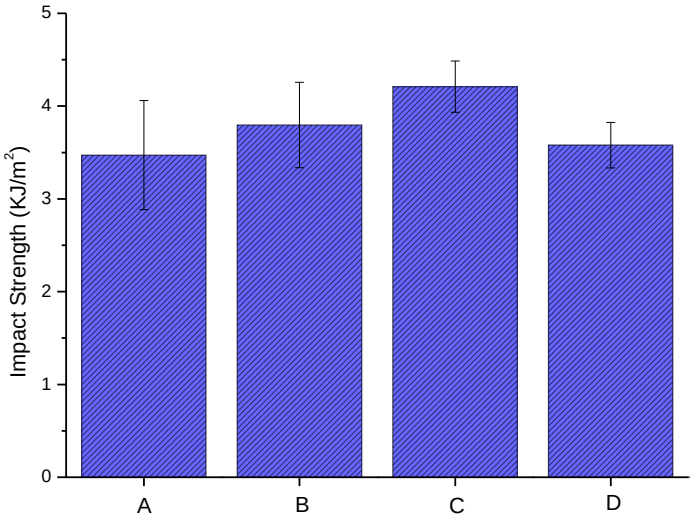

Figure 10. The Izod impact strength of various PP and HDPE samples; (A) neat PP, (B) PP blended with 5 wt.% NOUVEX N950-9010 MB, (C) Neat HDPE, and (D) HDPE blended with 5 wt.% NOUVEX N950-9010 MB.

The Izod impact strength (measured in KJ/m^2) for the melt-compounded PP with 5 wt.% of Nouvex N950-9010 MB was 3.797 ± 0.46, higher than the neat PP at 3.472 ± 0.59. The Izod impact strength for the melt-compounded HDPE with 5 wt.% of Nouvex N950-9010 MB was 3.579 ± 0.25 which was lower than the neat HDPE at 4.209 ± 0.28.

Overall, the addition of 5 wt.% of Nouvex N950-9010 MB slightly increased the impact strength of the modified PP samples, but slightly reduced for the strength of the modified HDPE, as shown in (**Figure 10**).

4.7.2. Tensile properties

The results of tensile tests on the PP and HDPE samples are presented in (**Figure 11**).

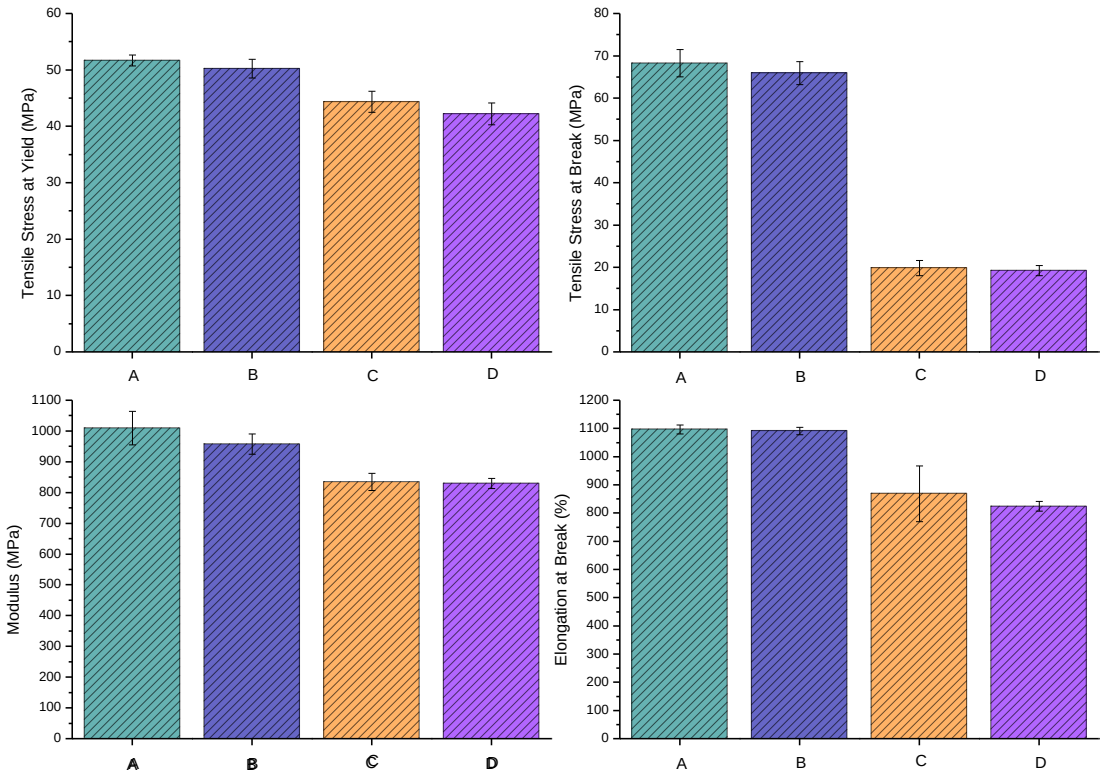

Figure 11. The tensile properties of each graph represent the following samples (on the x axis); (A) neat PP, (B) PP blended with 5 wt.% NOUVEX N950-9010 MB, (C) Neat HDPE, (D) HDPE blended with 5 wt.% NOUVEX N950-9010 MB.

The tensile properties of the four samples studied: neat PP, PP blended with 5 wt.% Nouvex N950-9010 MB, neat HDPE and HDPE blended with 5 wt.% Nouvex N950-9010 MB were evaluated in terms of their tensile stress at yield (measured in MPa), tensile stress at break (measured in MPa), modulus (measured in MPa) and elongation at break (measured in %).

The tensile stress at yield (measured in MPa) for the PP blended with 5 wt.% Nouvex N950-9010 M.S was 50.24 ± 1.55, which was slightly lower than that of the neat PP at 51.7 ± 0.99, whereas the HDPE blended with 5 wt.% Nouvex N950-9010 MB was 42.24 ± 1.97, which was also lower than its neat HDPE sample at 44.4 ± 1.87.

The tensile stress at break (measured in MPa) for the PP blended with 5 wt.% Nouvex N950-9010 MB was at 65.96 ± 2.72, which was lower than that of the neat PP at 68.30 ± 3.21. At the same time, the HDPE blended with 5 wt.% Nouvex N950-9010 MB was 19.25 ± 1.20, which was slightly lower than, but comparable with, its neat HDPE sample at 19.88 ± 1.80.

The modulus (measured in MPa) of the PP blended with 5 wt.% Nouvex N950-9010 MB was 958.09 ± 32.58, which was lower than the neat PP at 1010.01 ± 54.31, whereas the HDPE blended with 5 wt.% Nouvex N950-9010 MB was 830.05 ± 16.00, which was also lower than its neat HDPE sample at 835.09 ± 28.00.

The elongation at break (measured in %) of the PP blended with 5 wt.% Nouvex N950-9010 MB was 1091.78 ± 13.36, which was lower than that of the neat PP at 1097.30 ± 16.25, whereas the HDPE blended with 5 wt.% Nouvex N950-9010 MB was 824.63 ± 17.36 which was also lower than its neat HDPE sample at 868.90 ± 98.70.

Overall, the data obtained for the modified PP and HDPE samples were comparable with or lower than those for the neat PP and HDPE, as shown in (**Figure 11**).

4.8. UV–visible spectrophotometry — Leachability

The UV spectra for various PP and HDPE samples are presented in (**Figure 12**) which consists of two separate line graphs plotted on the same set of axes. The Y-axis represents absorbance, while the X-axis represents wavelength (nm). Each graph contains three lines, representing different materials or compositions. In both graphs, the black line represents a neat polymer (neat PP in the first graph and neat HDPE in the second). The red line represents a polymer mixed with NOUVEX N950-9010 MB (PP and HDPE, respectively). The blue line represents a polymer with 5 wt.% of NOUVEX N950-9010 MB added (PP and HDPE, respectively). Absorbance values range from 0 to approximately 0.7 for neat PP and 0 to approximately 0.8 for neat HDPE. Measurements were made at wavelengths from 200 nm to 400 nm. Both red lines indicating the pure NOUVEX MB N950-9010 pellets showed higher absorbance compared with their neat counterparts across all wavelengths.

The leachability evaluation results obtained using the UV light transmission method indicated that the neat PP and HDPE pellets, as well as their melt-compounding blends with 5 wt.% Nouvex N950-9010 MB, showed no significant difference in their leachability curves. Although the leachability for the raw Nouvex N950-9010 MB pure pellets showed some absorbance peaks in the range between 200 and 280 nm, once it was blended with PP and HDPE at 5 wt.% loading, the peaks disappeared, as shown in (**Figure 12**). This indicates that the Nouvex N950-9010 MB did not leach from the melt-compounded PP and HDPE pellets, which supports the manufacturer's claim that classified this MB as "non-leachable".[29]

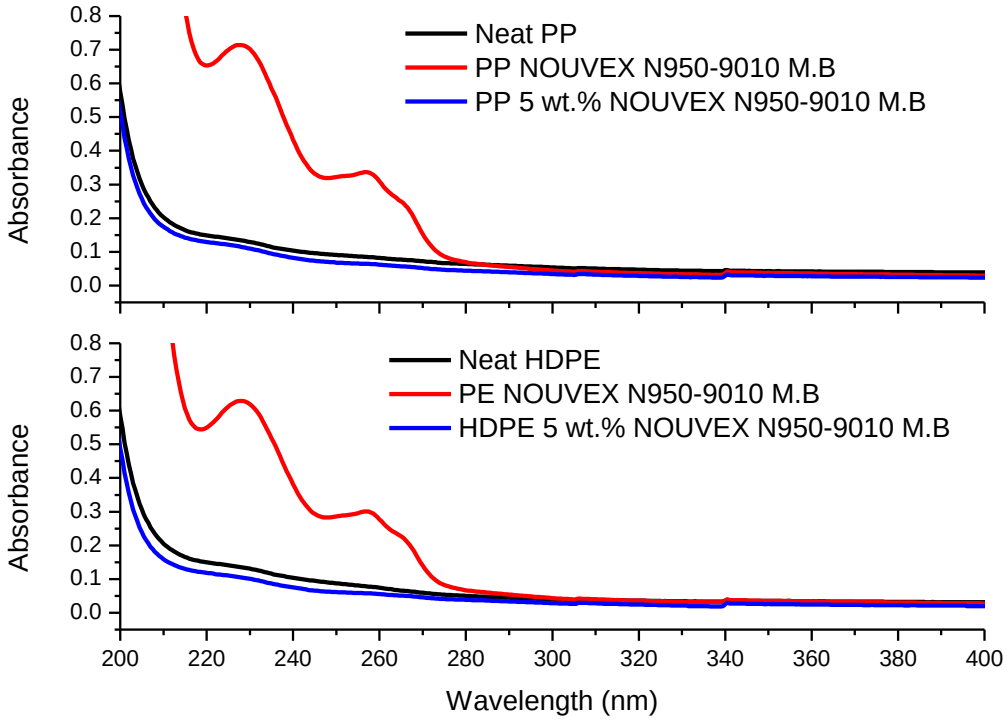

Figure 12. The UV spectra for various PP and HDPE samples.

4.9. Anti-microbial studies

The anti-microbial activities of *E. coli* K-12 MG1655 and *S. aureus* ATCC 6538P for various PP and HDPE samples are presented in (**Figure 13** and **Figure 14**).

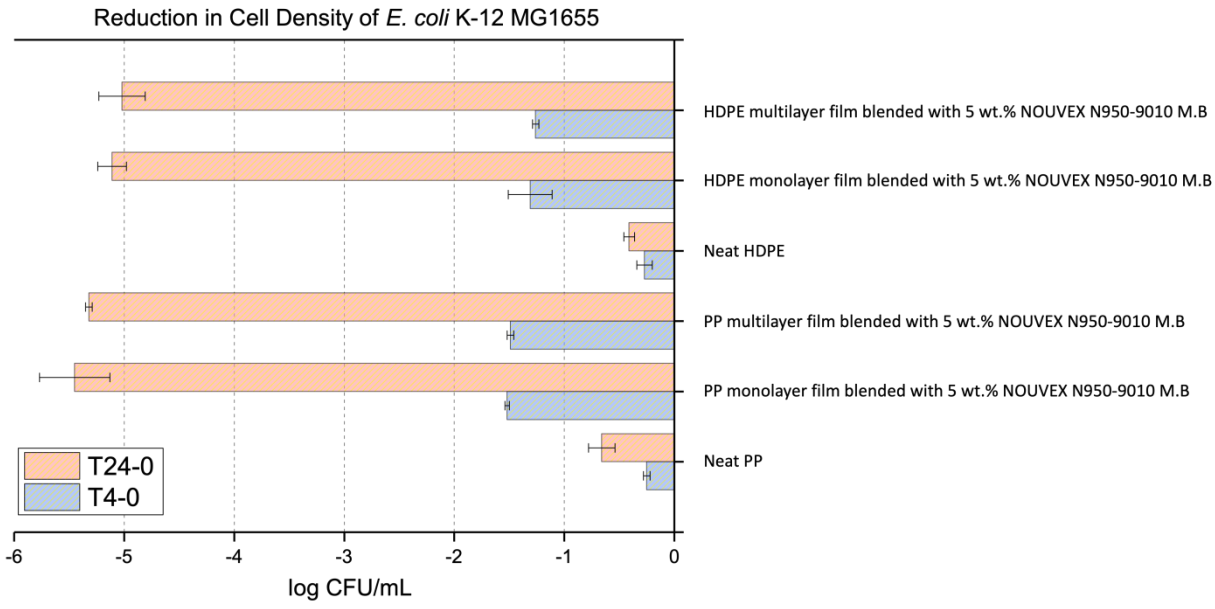

Figure 13. The anti-microbial activity of *E. coli* K-12 MG1655 for various PP and HDPE samples.

The anti-microbial results for the modified PP and HDPE samples against *E. coli* K-12 MG1655 (**Figure 13**) showed a significant reduction of the cell density (measured in log CFU/mL) over a period of 4 and 24 hours. It is noticeable that both melt-compounded and extruded PP and HDPE films as monolayer and multilayer were very comparable in their anti-microbial activity. The multilayer films were tested on the blended side of the 5 wt.% Nouvex N950-9010 MB.

For the PP blended with 5 wt.% Nouvex N950-9010 MS, the cell density reduction of the monolayer films was -1.52 ± 0.02 and -5.45 ± 0.32 log CFU/mL at 4- and 24-hour intervals, respectively. For the multilayer films of PP blended with 5 wt.% Nouvex N950-9010 MB, the cell density reduction was -1.49 ± 0.03 and -5.32 ± 0.03 log CFU/mL at 4- and 24-hour intervals, respectively. In both cases, the reduction in the cell density was enhanced compared with the neat PP films, which showed a decrease of -0.25 ± 0.03 and -0.66 ± 0.12 log CFU/mL at the 4- and 24-hour intervals, respectively.

In the case of HDPE blended with 5 wt.% Nouvex N950-9010 MB, the cell density reduction of the monolayer films was -1.31 ± 0.20 and -5.11 ± 0.13 log CFU/mL at the 4- and 24-hour intervals, respectively. For the multilayer films of HDPE blended with 5 wt.% Nouvex N950-9010 MB, the cell density reduction was -1.26 ± 0.03 and -5.02 ± 0.21 log CFU/mL at the 4- and 24-hour intervals, respectively. In both cases, the reduction in the cell density was enhanced compared with the neat HDPE films, which showed a reduction of -0.27 ± 0.07 and -0.41 ± 0.05 log CFU/mL at the 4- and 24-hour intervals, respectively.

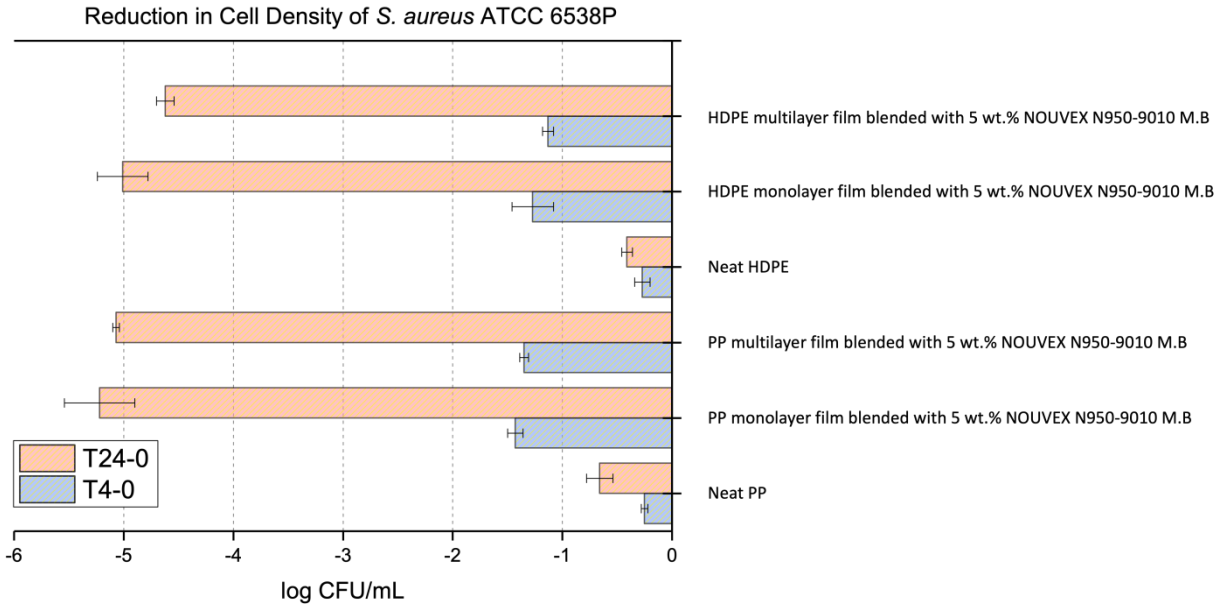

Figure 14. The anti-microbial activity of *S. aureus* ATCC 6538P for various PP and HDPE samples.

The anti-microbial data obtained for the modified PP and HDPE sample against *S. aureus* ATCC 6538P (**Figure 14**) showed a reduction of the cell density (measured in log CFU/mL) over a period of 4 and 24 hours. It is clearly seen that both melt-compounded and film extruded PP and HDPE films as monolayer and multilayer were also very comparable in their anti-microbial activity. The multilayer films were tested on the blended side of the 5 wt.% Nouvex N950-9010 MB.

For the PP blended with 5 wt.% Nouvex N950-9010 MB, the cell density reduction of the monolayer films was -1.43 ± 0.07 and -5.23 ± 0.32 log CFU/mL at the 4- and 24-hour intervals, respectively. For the multilayer films of PP blended with 5 wt.% Nouvex N950-9010 M.S, the cell density reduction was -1.35 ± 0.04 and -5.07 ± 0.03 log CFU/mL at the 4- and 24-hour intervals, respectively. In both cases, the reduction in the cell density was enhanced compared with the neat PP films, which showed a reduction of -0.25 ± 0.03 and -0.66 ± 0.12 log CFU/mL at the 4- and 24-hour intervals, respectively.

In the case of HDPE blended with 5 wt.% Nouvex N950-9010 M.S, the cell density reduction of the monolayer films was -1.27 ± 0.19 and -5.01 ± 0.23 log CFU/mL at the 4- and 24-hour intervals, respectively. For the multilayer films of HDPE blended with 5 wt.% Nouvex N950-9010 MB, the cell density reduction was -1.13 ± 0.05 and -4.62 ± 0.08 log CFU/mL at the 4- and 24-hour intervals, respectively. In both cases, the

reduction in the cell density was enhanced compared with the neat HDPE films, which showed a reduction of -0.27 ± 0.07 and -0.41 ± 0.05 log CFU/mL at the 4- and 24-hour intervals, respectively.

4.10. NOUVEX N950-9010 MB—Mode of action

The fluorescent images for various PP and HDPE samples are presented in (**Figure 15**).

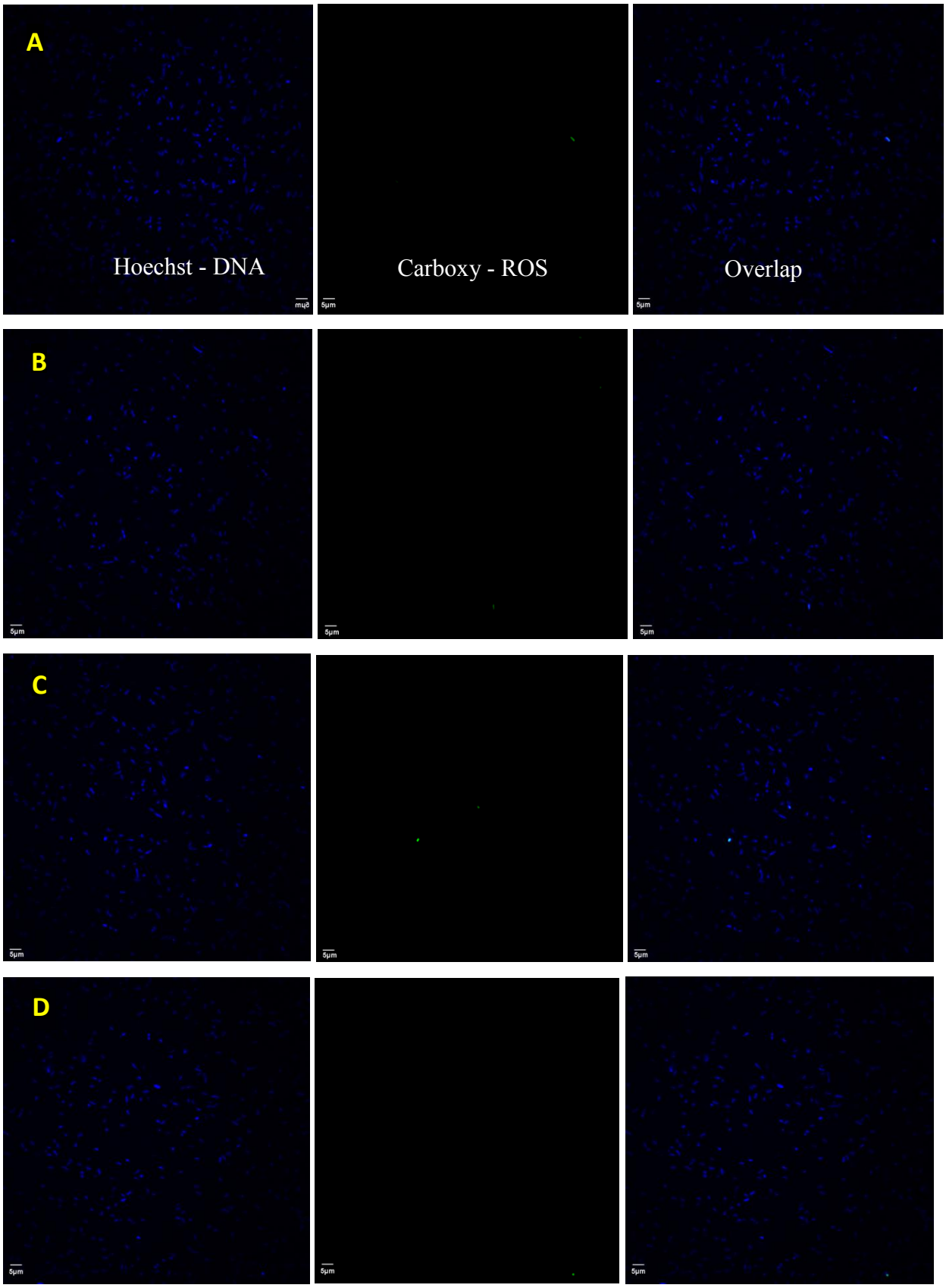

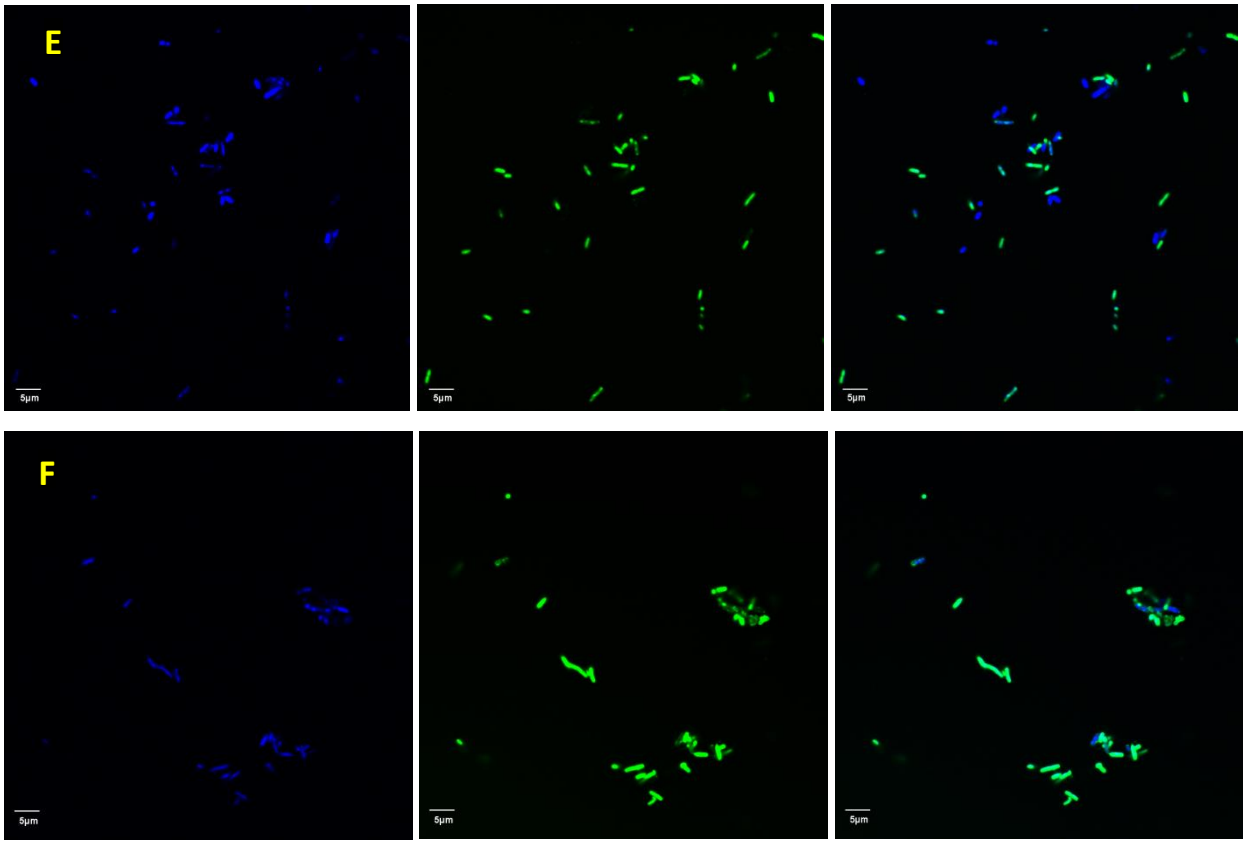

Figure 15. The fluorescent images for various PP and HDPE samples; (A) Neat bacterial suspension used for PP monolayer film, (B) Neat bacterial suspension used for HDPE monolayer film, (C) Bacterial suspension + neat monolayer PP film, (D) Bacterial suspension + neat monolayer HDPE film, and (E) Bacterial suspension + compounded monolayer PP film with 5 wt.% NOUVEX N950-9010 MB, (F) Bacterial suspension + compounded monolayer HDPE film with 5 wt.% NOUVEX N950-9010 MB.

The positive ROS bacteria (colored green) were evaluated and counted in six different suspensions: neat bacterial suspension used for PP monolayer film, neat bacterial suspension used for HDPE monolayer film, bacterial suspension + neat monolayer PP film, bacterial suspension + neat monolayer HDPE film, bacterial suspension + compounded monolayer PP film with 5 wt.% NOUVEX N950-9010 MB, and bacterial suspension + compounded monolayer HDPE film with 5 wt.% NOUVEX N950-9010 MB.

Regarding the neat bacterial suspension used for PP monolayer film and bacterial suspension + neat monolayer PP film, only a single bacterium was colored green, indicating a ROS count of 1, while in the case of neat bacterial suspension used for HDPE monolayer film and bacterial suspension + neat monolayer HDPE film, no reactivity was shown; ROS count of 0. However, the positive ROS bacteria of the bacterial suspension + compounded monolayer PP film with 5 wt.% NOUVEX N950-9010 MB, and bacterial suspension + compounded monolayer HDPE film with 5 wt.% NOUVEX N950-9010 MB, showed an average number of 45 and 35, respectively. The results are summarized in (**Table 4**).

Table 4. Average positive ROS bacterial count for neat and modified monolayer film PP and HDPE films.

Samples	Average positive ROS bacterial
Neat bacterial suspension used for PP monolayer film	1
Neat bacterial suspension used for HDPE monolayer film	0
Bacterial suspension + neat monolayer PP film	1
Bacterial suspension + neat monolayer HDPE film	0
Bacterial suspension + compounded monolayer PP film with 5 wt.% NOUVEX N950-9010 MB	45
Bacterial suspension + compounded monolayer HDPE film with 5 wt.% NOUVEX N950-9010 MB.	35

5. Conclusions

The anti-microbial efficacy of a novel organic-based anti-microbial master batch called Nouvex N950-9010 MB was evaluated when incorporated into PP and HDPE. The findings revealed remarkable activity against both *E. coli* K-12 MG1655 and *S. aureus* ATCC 6538P at two critical time intervals: 4 hours and 24 hours. The production process involved melt-compounding the Nouvex N950-9010 MB at 5 wt.% loading concentration with PP and HDPE, followed by extrusion into monolayer and multilayer films. SEM analysis demonstrated homogeneous mixing and excellent adhesion within the multilayer films. Thermal stability was confirmed through DSC and TGA, with all variations well within experimental error margins. Surprisingly, FTIR results indicated no significant differences between modified and neat materials, suggesting that Nouvex N950-9010 MB does not compromise material integrity of polyolefins. Stability was maintained in terms of MFI and density, with no substantial deviations observed. Notably, the modified PP and HDPE exhibited improved oxygen and water vapor barrier properties (OTR and WVTR) compared with their neat counterparts. Mechanical properties, including Izod impact and tensile strengths, remained stable for the modified materials. Furthermore, UV spectra confirmed the absence of leachability, aligning with the manufacturer's classification of Nouvex N950-9010 MB as non-leachable. Most intriguingly, the study elucidated the mode of action for Nouvex N950-9010 MB: it operates via reactive oxygen species (ROS), marking a pioneering discovery in the realm of novel anti-microbial agents. In summary, the investigation demonstrates the potential of Nouvex N950-9010 MB as a powerful and safe anti-microbial solution, opening new avenues for research and practical applications for the plastics industry.

Acknowledgements

The author expresses his gratitude to SABIC for generously funding his doctoral studies and research requirements at Michigan State University. He is indebted to Jérôme Vachon from Sabic T&I, and Craig Kalmer from Poly Group LLC for their help in proofreading the manuscript.

Conflict of Interest

The author has no conflicts of interest.

References

1. Meadow, J. F.; Altrichter, A. E.; Kembel, S. W.; Moriyama, M.; O'Connor, T. K.; Womack, A. M.; Brown, G.; Green, J. L.; Bohannan, B. J. J. M. Bacterial communities on classroom surfaces vary with human contact. 2014, 2, 1-7.
2. Guglielmi, G. Bacteria navigate on surfaces using a 'sense of touch'. 2021, Research News. (acccessed December 2023).
3. Ahveninen, A. How germs spread from surfaces. (acccessed December 2023).
4. Microbiology, S. Routes of transmission.
5. Alkarri, S. Investigate the Effect of Coating Concentration and Coating Thickness on the Anti-microbial Properties of Polycarbonate Sheet. 2024.
6. Li, D.; Zhou, L.; Wang, X.; He, L.; Yang, X. J. M. Effect of crystallinity of polyethylene with different densities on breakdown strength and conductance property. 2019, 12 (11), 1746.
7. Watson, R.; Oldfield, M.; Bryant, J. A.; Riordan, L.; Hill, H. J.; Watts, J. A.; Alexander, M. R.; Cox, M. J.; Stamataki, Z.; Scurr, D. J. J. S. R. Efficacy of antimicrobial and anti-viral coated air filters to prevent the spread of airborne pathogens. 2022, 12 (1), 2803.
8. Hammond, A.; Khalid, T.; Thornton, H. V.; Woodall, C. A.; Hay, A. D. J. P. O. Should homes and workplaces purchase portable air filters to reduce the transmission of SARS-CoV-2 and other respiratory infections? A systematic review. 2021, 16 (4), e0251049.
9. Alkarri, S.; Vachon, J. Relationship between Particle Size, Anti-Microbial Activity and Leachability of Copper Particles in Liquid Suspension and Compounded in Polypropylene. Annals of Biomedical Science and Engineering 2024, 8 (1), 021-031.
10. Grinberg, M.; Orevi, T.; Kashtan, N. Bacterial surface colonization, preferential attachment and fitness under periodic stress. PLOS Computational Biology 2019, 15 (3), e1006815. DOI: 10.1371/journal.pcbi.1006815.

11. Lo, L. S. H.; Liu, X.; Qian, P.-Y.; Häggblom, M. M.; Cheng, J. Microbial colonization and chemically influenced selective enrichment of bacterial pathogens on polycarbonate plastic. Environmental Science and Pollution Research 2024, 31 (5), 8061-8071. DOI: 10.1007/s11356-023-31752-6.
12. Klassert, T. E.; Leistner, R.; Zubiria-Barrera, C.; Stock, M.; López, M.; Neubert, R.; Driesch, D.; Gastmeier, P.; Slevogt, H. Bacterial colonization dynamics and antibiotic resistance gene dissemination in the hospital environment after first patient occupancy: a longitudinal metagenetic study. Microbiome 2021, 9 (1), 169. DOI: 10.1186/s40168-021-01109-7.
13. Kramer, A.; Assadian, O. J. U. o. b. s. f. r. o. h. a. i. Survival of microorganisms on inanimate surfaces. 2014, 7-26.
14. Contributors to Wikimedia, p. Antimicrobial surface.
15. The surfaces that kill bacteria and viruses. BBC, 2020. https://www.bbc.com/future/article/20200529-the-surfaces-that-kill-bacteria-and-viruses (accessed 2024/3/31/).
16. Birkett, M.; Dover, L.; Cherian Lukose, C.; Wasy Zia, A.; Tambuwala, M. M.; Serrano-Aroca, Á. Recent Advances in Metal-Based Antimicrobial Coatings for High-Touch Surfaces. 2022, 23 (3), 1162.
17. Luo, H.; Yin, X.-Q.; Tan, P.-F.; Gu, Z.-P.; Liu, Z.-M.; Tan, L. Polymeric antibacterial materials: design, platforms and applications. Journal of Materials Chemistry B 2021, 9 (12), 2802-2815, 10.1039/D1TB00109D. DOI: 10.1039/D1TB00109D.
18. Skwarczynski, M.; Bashiri, S.; Yuan, Y.; Ziora, Z. M.; Nabil, O.; Masuda, K.; Khongkow, M.; Rimsueb, N.; Cabral, H.; Ruktanonchai, U.; et al. Antimicrobial Activity Enhancers: Towards Smart Delivery of Antimicrobial Agents. 2022, 11 (3), 412.
19. Alkarri, S. Developing Methods for Incorporating Antimicrobial Biocidal Nanoparticles in Thermoplastics. Michigan State University, 2023.
20. Poly, G. Poly Group LLC - Nouvex Antimicrobial.
21. Purdue News, S. Novel antimicrobial polymer receives EPA approval.
22. Programs, U. S. E. P. A. O. o. P. US EPA, pesticide product label, NOUVEX N950-9010 MASTER BATCH,03/22/2017. United states environmental protection agency Decision No. 526851 (EPA Reg. No. 91413-2). (acccessed 2024/3/31/).
23. Brandrup, J.; Immergut, E. H.; Grulke, E. A.; Abe, A.; Bloch, D. R. Polymer handbook; Wiley New York, 1999.
24. Li, D.; Zhou, L.; Wang, X.; He, L.; Yang, X. Effect of Crystallinity of Polyethylene with Different Densities on Breakdown Strength and Conductance Property. Materials (Basel, Switzerland) 2019, 12 (11). DOI: 10.3390/ma12111746 From NLM.
25. Alkarri, S.; Bin Saad, H.; Soliman, M. On Antimicrobial Polymers: Development, Mechanism of Action, International Testing Procedures, and Applications. Polymers 2024, 16 (6), 771.
26. Čapek, J.; Roušar, T. Detection of oxidative stress induced by nanomaterials in cells—the roles of reactive oxygen species and glutathione. Molecules 2021, 26 (16), 4710.
27. Saleh, A.; Melinda, F.; John, C.; Lee, M.; Jin H, K.; Jonathan O, R. Investigating anti-bacterial and anti-covid-19 virus properties and mode of action of pure mg(oh)2 and copper-infused mg(oh)2 nanoparticles and coated polypropylene surfaces. Int J Clin Virol 8 (1), 008-023. DOI: 10.29328/journal.ijcv.1001057 (acccessed 2024/6/18/).
28. Gu, J.; Xu, H.; Wu, C. J. A. i. p. t. Thermal and crystallization properties of HDPE and HDPE/PP blends modified with DCP. 2014, 33 (1).
29. Alkarri, S.; Sharma, D.; Bergholz, T. M.; Rabnawaz, M. J. J. o. A. P. S. Fabrication methodologies for antimicrobial polypropylene surfaces with leachable and nonleachable antimicrobial agents. 2024, 141 (1), e54757.